

# Synthesis, structure, spectroscopic properties and cytotoxic effect of some thiosemicarbazone complexes of palladium†

Sarmistha Halder,<sup>a</sup> Shie-Ming Peng,<sup>b</sup> Gene-Hsiang Lee,<sup>b</sup> Tanmay Chatterjee,<sup>c</sup> Asama Mukherjee,<sup>d</sup> Sushanta Dutta,<sup>d</sup> Utpal Sanyal<sup>d</sup> and Samaresh Bhattacharya<sup>\*a</sup>

Received (in Montpellier, France) 17th May 2007, Accepted 21st August 2007

First published as an Advance Article on the web 6th September 2007

DOI: 10.1039/b707448d

Reaction of salicylaldehyde thiosemicarbazone ( $H_2L^1$ ), 2-hydroxyacetophenone thiosemicarbazone ( $H_2L^2$ ) and 2-hydroxynaphthaldehyde thiosemicarbazone ( $H_2L^3$ ) (general abbreviation  $H_2L$ , where  $H_2$  stands for the two dissociable protons, one phenolic proton and one hydrazinic proton) with  $Na_2[PdCl_4]$  affords a family of polymeric complexes of type  $[Pd(L)]_n$ . Reaction of the polymeric species with two monodentate ligands (D), viz. triphenylphosphine ( $PPh_3$ ) and 4-picoline (pic), has yielded complexes of type  $[Pd(L)(D)]$ . These mixed-ligand complexes have also been obtained from reaction of the thiosemicarbazones with  $[Pd(PPh_3)_2Cl_2]$  and  $[Pd(pic)_2Cl_2]$ . Crystal structures of  $[Pd(L^1)(PPh_3)]$  and  $[Pd(L^2)(pic)]$  have been determined. The  $[Pd(L)(D)]$  complexes show characteristic  $^1H$  NMR spectra and intense absorptions in the visible and ultraviolet region. They also fluoresce in the visible region at ambient temperature. *In vitro* cytotoxicity screenings of the complexes along with four human clinical drugs viz. cisplatin, BCNU, 5-fluorouracil (5-FU) and hydroxyurea have been carried out in two human tumor cell lines, namely promyelocytic leukemia HL-60 and histiocytic lymphoma U-937.  $[Pd(L^2)(PPh_3)]$  shows the lowest  $IC_{50}$  value and is found to be much more cytotoxic than the reference anticancer drugs in both the cell lines. An apoptosis study in HL-60 with  $[Pd(L^2)(PPh_3)]$  confirms that at 10  $\mu M$  concentration it induces apoptosis to a greater extent than cisplatin and camptothecin.

## 1. Introduction

The chemistry of transition metal complexes of thiosemicarbazones has received considerable attention, largely because of their bioinorganic relevance.<sup>1</sup> Such complexes are of particular importance due to their potentially beneficial biological (viz. antibacterial, antimalarial, antiviral and antitumor) activities.<sup>2</sup> Thiosemicarbazones usually bind to a metal ion, via dissociation of the hydrazinic proton, as bidentate N,S-donors, forming a five-membered chelate ring (1).<sup>3</sup> If a third donor site (D) is incorporated in such ligands, linked to the carbonylic carbon via one or two intervening atoms, then D,N,S-tricoordination (2) normally takes place.<sup>4</sup> In addition to displaying D,N,S-tricoordination, such ligands are also known to bridge a second metal ion through the sulfur.<sup>5</sup> It has also been observed that salicylaldehyde thiosemicarbazone, in spite of

having the phenolic oxygen as a potential third donor site, coordinates as a bidentate N,S-donor, forming a rather unusual four-membered chelate ring (3).<sup>6</sup> This mode of binding (3) has also been displayed by some other thiosemicarbazones.<sup>7</sup> Formation of such a chelate ring (3) by salicylaldehyde thiosemicarbazone, leaving some potential donor sites unused, has been utilized successfully in the synthesis of an interesting polynuclear complex.<sup>8</sup> This variable binding mode of thiosemicarbazones has encouraged us to explore their coordination chemistry further,<sup>6,8,9</sup> and the present work has originated from this exploration. Herein we have chosen three potentially tridentate thiosemicarbazones, viz. the thiosemicarbazones of salicylaldehyde, 2-hydroxyacetophenone and 2-hydroxynaphthaldehyde. These thiosemicarbazones are abbreviated in general as  $H_2L$ , where  $H_2$  stands for the two dissociable protons, the phenolic proton and the hydrazinic proton. Individual ligand abbreviations are shown in 4. To interact with the chosen thiosemicarbazones, palladium has been selected as the metal. It may be mentioned here that, though the chemistry of palladium complexes of some thiosemicarbazones has been studied,<sup>10</sup> that of the chosen thiosemicarbazones (4) appears to have remained unexplored. Reaction of the three selected thiosemicarbazones (4) has been carried out with three palladium starting materials, viz.  $Na_2[PdCl_4]$ ,  $[Pd(PPh_3)_2Cl_2]$  and  $[Pd(pic)_2Cl_2]$  (pic = 4-picoline), which has afforded a family of interesting complexes containing the thiosemicarbazones coordinated in the tridentate fashion (5). The chemistry of these complexes is reported in this paper with special reference to their synthesis, structure and spectral

<sup>a</sup> Department of Chemistry, Inorganic Chemistry Section, Jadavpur University, Kolkata 700 032, India. E-mail: samaresh\_b@yahoo.com

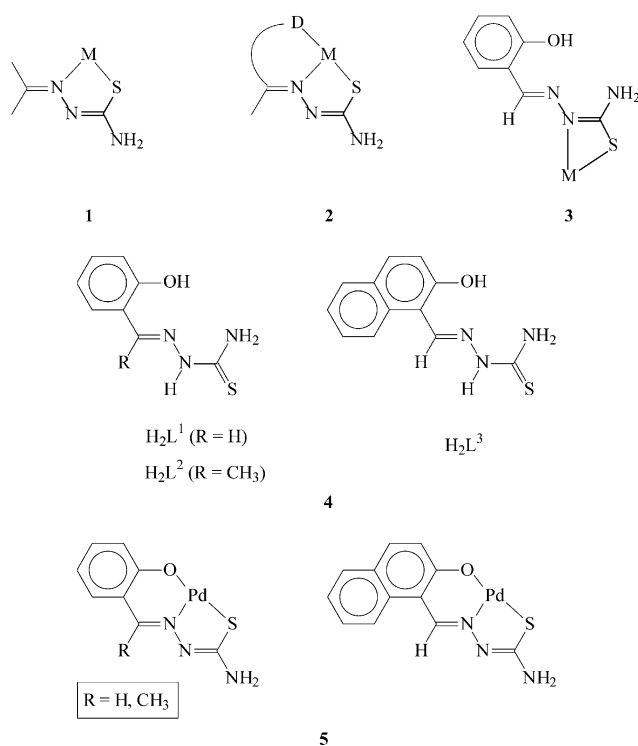
<sup>b</sup> Department of Chemistry, National Taiwan University, Taipei, Taiwan, ROC

<sup>c</sup> School of Chemistry, University of Hyderabad, Hyderabad 500 046, India

<sup>d</sup> Department of Anticancer Drug Development, Chittaranjan National Cancer Institute, Kolkata 700 026, India

† Electronic supplementary information (ESI) available: A diagram showing metal- $\pi$  interaction in the  $[Pd(L)(PPh_3)]$  complex (Fig. S1), a diagram showing  $\pi$ - $\pi$  interaction in the  $[Pd(L)(pic)]$  complex (Fig. S2), a table showing metal- $\pi$  and  $\pi$ - $\pi$  interactions in the  $[Pd(L)(PPh_3)]$  and  $[Pd(L)(pic)]$  complexes, respectively (Table S1) and a partial MO diagram of the  $[Pd(L)(pic)]$  complex (Fig. S3). See DOI: 10.1039/b707448d

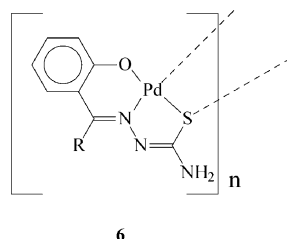
properties, and cytotoxic activity in two human tumor cell lines.



## Results and discussion

### Syntheses

Reaction of the selected thiosemicarbazones ( $H_2L$ , **4**) has been carried out first with  $Na_2[PdCl_4]$  in refluxing ethanol in the presence of triethylamine to afford a family of polymeric complexes of type  $[Pd(L)]_n$  in decent yields. Based on the compositions of these complexes, as well as the +2 oxidation state of palladium in them, the thiosemicarbazones are believed to coordinate the metal center in the expected dianionic O,N,S-fashion (**5**). The fourth coordination position on palladium in the  $Pd(L)$  fragment is assumed to be taken up by the sulfur of a coordinated thiosemicarbazone belonging to another  $Pd(L)$  fragment (**6**). This bridging action of the thiosemicarbazone sulfur, which is well documented in the literature,<sup>5</sup> appears to be responsible for the formation of the polymeric species.

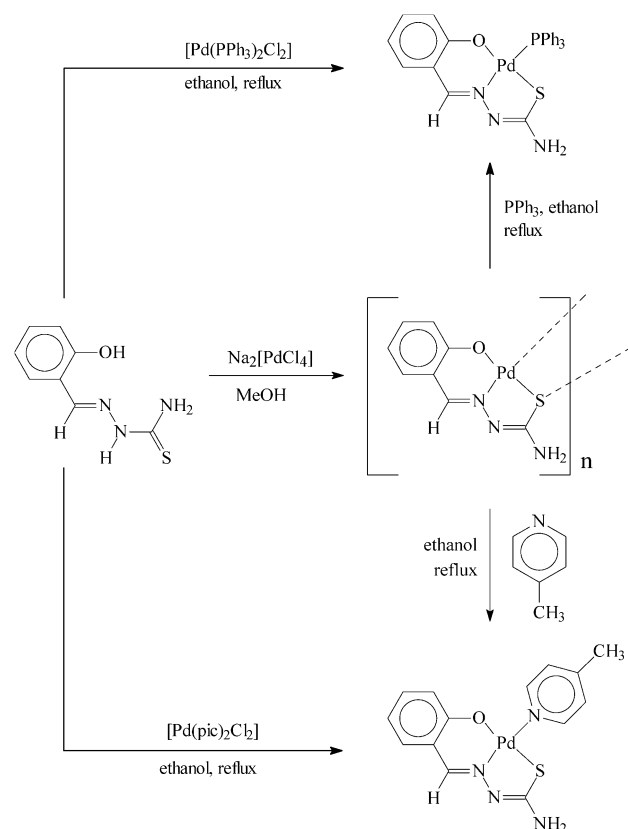


In order to explore the possibility of forming monomeric complexes by splitting the sulfur bridge in the  $[Pd(L)]_n$  complexes, their reaction has been carried out with two monodentate ligands (D), viz. triphenylphosphine ( $PPh_3$ ) and 4-picoline (pic). From each of these reactions a monomeric

complex of type  $[Pd(L)(D)]$  ( $D = PPh_3$  or pic) has been obtained. The same monomeric complexes have also been synthesized, in better yields, by reaction of the thiosemicarbazones (**4**) with  $[Pd(PPh_3)_2Cl_2]$  and  $[Pd(pic)_2Cl_2]$  in refluxing ethanol in the presence of triethylamine. Synthetic methods for all the complexes are illustrated in Scheme 1. The observed elemental (C, H, N) analytical data of the synthesized complexes are found to be consistent with their compositions.

### Crystal structures

In order to authenticate the coordination modes of the thiosemicarbazones in these monomeric  $[Pd(L)(D)]$  complexes, structures of a representative member from each family, viz.  $[Pd(L^1)(PPh_3)]$  and  $[Pd(L^2)(pic)]$ , have been determined by X-ray crystallography. The structure of the  $[Pd(L^1)(PPh_3)]$  complex is shown in Fig. 1 and some relevant bond parameters are listed in Table 1. The structure shows that the thiosemicarbazone ligand is coordinated to palladium in the expected tridentate fashion (**5**), forming six- and five-membered chelate rings with O–Pd–N and N–Pd–S bite angles of  $92.82(7)^\circ$  and  $84.26(5)^\circ$ , respectively. A triphenylphosphine is also coordinated to the metal center, which is *trans* to the nitrogen. Palladium is thus nested in an ONSP core, which is slightly distorted from ideal square planar geometry, as reflected in the bond parameters around the metal center. The Pd–O, Pd–N, Pd–S and Pd–P distances are all quite normal, as observed in structurally characterized complexes of palladium containing these bonds.<sup>10</sup> Bond distances within the coordinated thiosemicarbazone are also usual.<sup>9c</sup>



Scheme 1

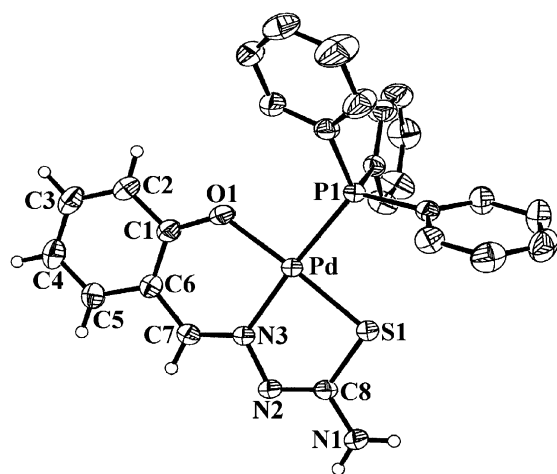


**Fig. 1** Structure of the  $[\text{Pd}(\text{L}^1)(\text{PPh}_3)]$  complex drawn at the 50% probability level.

The absence of any solvent of crystallization in the crystal lattice of  $[\text{Pd}(\text{L}^1)(\text{PPh}_3)]$  indicates the possible existence of non-covalent interaction(s) between the individual complex molecules. A closer look at the packing pattern of in the crystal reveals that hydrogen bonding interactions of two types, *viz.* intramolecular  $\text{C}-\text{H}\cdots\text{O}$  and intermolecular  $\text{N}-\text{H}\cdots\text{N}$ , are active in the lattice. A selected view of the hydrogen bonding interactions is shown in Fig. 2 and some hydrogen bond parameters are given in Table 2. One *ortho*  $\text{C}-\text{H}$  of a phenyl ring of the  $\text{PPh}_3$  is intramolecularly hydrogen bonded to the phenolate oxygen of the thiosemicarbazone ligand. One  $-\text{NH}_2$  hydrogen of each complex molecule is hydrogen bonded to the nitrogen next to the azomethine nitrogen of a second molecule and thus a hydrogen bonded dimer is formed. Apart from these hydrogen bonding interactions, there also exist  $\text{Pd}-\pi$  interactions between the metal center of one complex molecule and the phenyl ring of the thiosemicarbazone ligand of a second complex molecule (Fig. S1, Table S1†). This extended  $\text{Pd}-\pi$  interaction seems to be responsible for holding the crystal together. It may be relevant

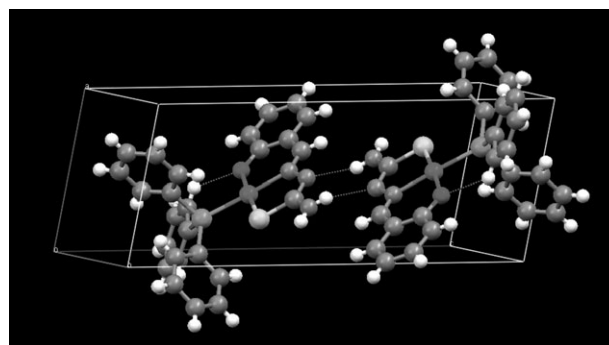


**Fig. 2** Hydrogen bonding interactions in the lattice of  $[\text{Pd}(\text{L}^1)(\text{PPh}_3)]$ .

to note here that such non-covalent interactions are of significant importance in molecular recognition processes as well as in crystal engineering.<sup>11</sup>

The structure of the  $[\text{Pd}(\text{L}^2)(\text{pic})]$  complex (Fig. 3) shows that the thiosemicarbazone ligand is coordinated to palladium in the same tridentate fashion (**5**) as in  $[\text{Pd}(\text{L}^1)(\text{PPh}_3)]$ , and a 4-picoline has taken up the fourth coordination site on the metal center. In this complex palladium has an ONSN coordination sphere around it. The observed  $\text{Pd}-\text{N}(\text{pic})$  distance is normal,<sup>12</sup> and the structural features in the  $\text{Pd}(\text{L}^2)$  fragment are similar to those observed in the  $\text{Pd}(\text{L}^1)$  fragment of the  $[\text{Pd}(\text{L}^1)(\text{PPh}_3)]$  complex. An examination of the packing pattern in this  $[\text{Pd}(\text{L}^2)(\text{pic})]$  crystal shows that three intramolecular hydrogen bonding interactions, *viz.*  $\text{C}-\text{H}\cdots\text{O}$ ,  $\text{C}-\text{H}\cdots\text{S}$  and  $\text{C}-\text{H}\cdots\text{N}$ , and one intermolecular hydrogen bonding interaction, *viz.*  $\text{N}-\text{H}\cdots\text{O}$ , are active in the lattice (Fig. 4, Table 2). Two picolyl  $\text{C}-\text{H}$ s (at the 2 and 6 positions) are intramolecularly hydrogen bonded to the phenolate oxygen and sulfur of the thiosemicarbazone ligand. One methyl  $\text{C}-\text{H}$  of the thiosemicarbazone is also intramolecularly hydrogen bonded to the nitrogen (which is not bound to the metal center) of the same ligand. One  $-\text{NH}_2$  hydrogen of each complex molecule is hydrogen bonded to the phenolate oxygen of a second molecule; this intermolecular hydrogen bonding has propagated along the *b*-axis through the lattice. Besides these hydrogen bonding interactions, there also exist  $\pi-\pi$  interactions between the picolyl rings and also between the picolyl and phenyl rings of the thiosemicarbazone ligand (Fig. S2, Table S1†). The extended intermolecular interactions have been responsible for holding the crystal together.

**Table 1** Selected bond distances and bond angles for  $[\text{Pd}(\text{L}^1)(\text{PPh}_3)]$  and  $[\text{Pd}(\text{L}^2)(\text{pic})]$

$[\text{Pd}(\text{L}^1)(\text{PPh}_3)]$			
Bond distances/Å			
$\text{Pd}-\text{N}(3)$	2.0147(17)	$\text{C}(8)-\text{N}(1)$	1.354(3)
$\text{Pd}-\text{P}$	2.2711(5)	$\text{C}(7)-\text{N}(3)$	1.290(3)
$\text{Pd}-\text{S}$	2.2411(6)	$\text{C}(1)-\text{O}(1)$	1.306(3)
$\text{Pd}-\text{O}(1)$	2.0157(16)	$\text{N}(2)-\text{N}(3)$	1.397(2)
		$\text{C}(8)-\text{S}$	1.748(2)
Bond angles/°			
$\text{N}(3)-\text{Pd}-\text{P}$	173.95(5)	$\text{N}(3)-\text{Pd}-\text{O}(1)$	92.82(7)
$\text{O}(1)-\text{Pd}-\text{S}(1)$	177.07(5)	$\text{N}(3)-\text{Pd}-\text{S}$	84.26(5)
$[\text{Pd}(\text{L}^2)(\text{pic})]$			
Bond distances/Å			
$\text{Pd}(1)-\text{N}(3)$	1.9861(15)	$\text{C}(8)-\text{N}(1)$	1.359(3)
$\text{Pd}(1)-\text{N}(4)$	2.0698(18)	$\text{C}(7)-\text{N}(3)$	1.309(2)
$\text{Pd}(1)-\text{S}(1)$	2.2510(7)	$\text{C}(1)-\text{O}(1)$	1.321(2)
$\text{Pd}(1)-\text{O}(1)$	1.9981(14)	$\text{N}(2)-\text{N}(3)$	1.397(2)
		$\text{C}(8)-\text{S}(1)$	1.736(2)
Bond angles/°			
$\text{N}(3)-\text{Pd}1-\text{N}(4)$	179.16(6)	$\text{N}(3)-\text{Pd}1-\text{O}(1)$	91.74(7)
$\text{O}(1)-\text{Pd}1-\text{S}(1)$	175.69(5)	$\text{N}(3)-\text{Pd}1-\text{S}(1)$	85.04(5)

**Table 2** Hydrogen bond distances and bond angles for  $[\text{Pd}(\text{L}^1)(\text{PPh}_3)]$  and  $[\text{Pd}(\text{L}^2)(\text{pic})]$ <sup>a</sup>

	Bond distances/Å			Bond angles/°
[Pd(L <sup>1</sup> )(PPh <sub>3</sub> )]				
N1–H1A···N2 <sup>i</sup>	0.86	2.18	3.004(3)	160
C10–H10A···O1	0.93	2.35	3.025(4)	130
[Pd(L <sup>2</sup> )(pic)]				
N1–H2N···O1 <sup>ii</sup>	0.86	2.24	2.888(2)	132
C9–H9A···N2	0.96	2.25	2.621(3)	102
C10–H10···S1	0.93	2.66	3.246(2)	122
C14–H14···O1	0.93	2.26	2.829(3)	119

<sup>a</sup> Symmetry: *i* = 1 – *x*, 2 – *y*, 1 – *z*; *ii* =  $\frac{1}{2}$  – *x*,  $\frac{1}{2}$  + *y*, *z*.

<sup>a</sup> Symmetry:  $i = 1 - x, 2 - y, 1 - z$ ;  $ii = \frac{1}{2} - x, \frac{1}{2} + y, z$ .

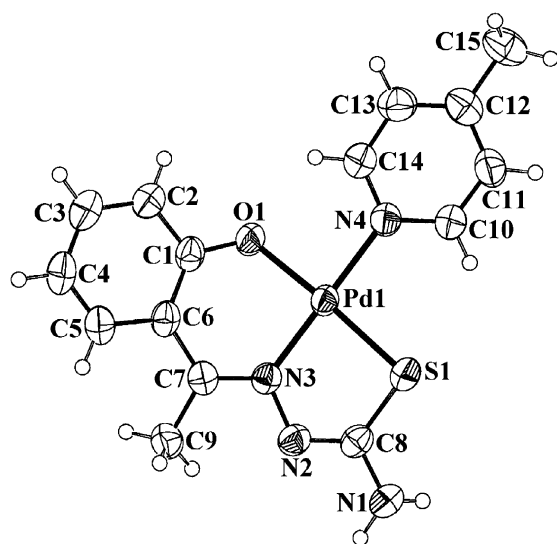


**Fig. 3** Structure of the  $[\text{Pd}(\text{L}^2)(\text{pic})]$  complex drawn at the 50% probability level.

### Spectral properties

$^1\text{H}$  NMR spectra of the  $[\text{Pd}(\text{L})(\text{PPh}_3)]$  complexes, recorded in  $\text{CDCl}_3$  solutions, show all the expected signals. Broad signals for the  $\text{PPh}_3$  ligands are observed within 7.4–7.8 ppm. In the  $[\text{Pd}(\text{L}^1)(\text{PPh}_3)]$  and  $[\text{Pd}(\text{L}^3)(\text{PPh}_3)]$  complexes the azomethine proton signal of the coordinated thiosemicarbazone is observed at 8.24 and 9.52 ppm, respectively. The methyl signal from the coordinated thiosemicarbazone in the  $[\text{Pd}(\text{L}^2)(\text{PPh}_3)]$  complex is observed at 2.89 ppm. The  $\text{NH}_2$  signal of the coordinated thiosemicarbazone is observed around 4.8 ppm. Most of the expected signals from the aryl fragment of the coordinated thiosemicarbazone are clearly observed in the aromatic region, while few could not be detected due to their overlap with other signals. In the  $^1\text{H}$  NMR spectra of the  $[\text{Pd}(\text{L})(\text{pic})]$  complexes, the methyl signal of the coordinated 4-picoline is observed at around 2.4 ppm and a distinct doublet is observed near 8.6 ppm, which is attributable to the  $\alpha$ -proton of the picoline. The other expected doublet for

the  $\beta$ -proton of the picoline is observed at 7.24 ppm in the  $[\text{Pd}(\text{L}^1)(\text{pic})]$  complex, but the same signal could not be detected in the other two complexes because of overlap problems. The  $^1\text{H}$  NMR spectral features for the coordinated thiosemicarbazones in these  $[\text{Pd}(\text{L})(\text{pic})]$  complexes are qualitatively similar to those observed for the corresponding  $[\text{Pd}(\text{L})(\text{PPh}_3)]$  complexes. The  $^1\text{H}$  NMR spectral data of the  $[\text{Pd}(\text{L})(\text{PPh}_3)]$  and  $[\text{Pd}(\text{L})(\text{pic})]$  complexes are therefore consistent with their compositions.

Infrared spectra of all the  $[\text{Pd}(\text{L})(\text{PPh}_3)]$  complexes show many vibrations of different intensities in the 1600–400  $\text{cm}^{-1}$  region. Assignment of each individual band to a specific vibration has not been attempted. However, three strong bands displayed near 533, 694 and 743  $\text{cm}^{-1}$  by these complexes, are attributed to the coordinated  $\text{PPh}_3$  ligands. Comparison with the spectrum of  $[\text{Pd}(\text{PPh}_3)_2\text{Cl}_2]$  shows the presence of several new bands (e.g. near 811, 1130, 1229, 1285, 1346, 1562 and 1599  $\text{cm}^{-1}$ ) in the spectra of the  $[\text{Pd}(\text{L})(\text{PPh}_3)]$  complexes, which must be due to the presence of the coordinated thiosemicarbazone ligand. Besides the absence of the three diagnostic bands for the  $\text{PPh}_3$  ligands near 533, 694 and 743  $\text{cm}^{-1}$ , infrared spectral properties of the  $[\text{Pd}(\text{L})(\text{pic})]$  complexes are qualitatively similar to those of the  $[\text{Pd}(\text{L})(\text{PPh}_3)]$  complexes.

The  $[\text{Pd}(\text{L})(\text{PPh}_3)]$  and  $[\text{Pd}(\text{L})(\text{pic})]$  complexes are soluble in common organic solvents such as methanol, ethanol, acetone, acetonitrile, dichloromethane, chloroform, *etc.*, producing intense yellow solutions. Electronic spectra of these complexes have been recorded in dichloromethane solution. Spectral data are presented in Table 3 and a selected spectrum is shown in Fig. 5. All the mixed-ligand complexes show several intense absorptions in the visible and ultraviolet regions. The absorptions in the ultraviolet region are assignable to transitions within the ligand orbitals and those in the visible region are probably due to charge-transfer transitions involving both metal and ligand orbitals. To have an understanding of the nature of the transitions in the visible region, qualitative extended Hückel molecular orbital (EHMO) calculations have been performed<sup>13</sup> on computer generated models of the  $[\text{Pd}(\text{L})(\text{PPh}_3)]$  and  $[\text{Pd}(\text{L})(\text{pic})]$  complexes. The results obtained are found to be similar for the three members of each group. A partial MO diagram for a representative  $[\text{Pd}(\text{L})(\text{PPh}_3)]$  complex is shown in Fig. 6 and that of a selected

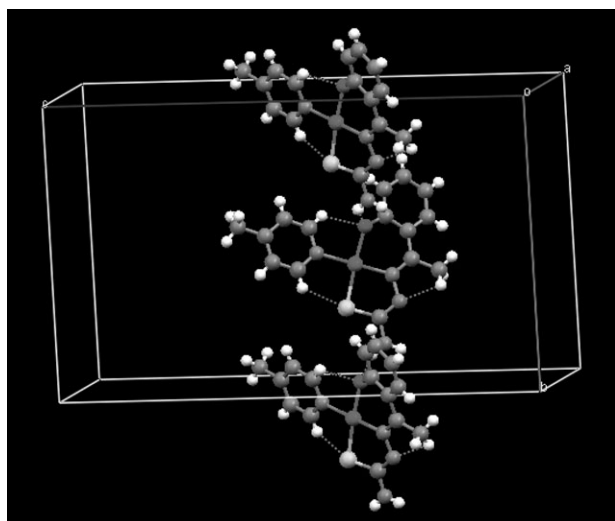


**Fig. 4** Hydrogen bonding interactions in the lattice of  $[\text{Pd}(\text{L}^2)(\text{pic})]$ .

**Table 3** Electronic spectral data in dichloromethane solution

Compound	$\lambda_{\text{max}}/\text{nm}$ ( $\epsilon/\text{dm}^3 \text{ mol}^{-1} \text{ cm}^{-1}$ ) <sup>a</sup>
$[\text{Pd}(\text{L}^1)(\text{PPh}_3)]$	398(9000), 342(11 300) <sup>s</sup> , 315(15 500), 298(16 100)
$[\text{Pd}(\text{L}^2)(\text{PPh}_3)]$	389(9800), 340(12 600) <sup>s</sup> , 313(19 000), 298(16 800)
$[\text{Pd}(\text{L}^3)(\text{PPh}_3)]$	430(9800), 408(9500), 389(5800) <sup>s</sup> , 348(12 000), 317(19 400), 261(41 300)
$[\text{Pd}(\text{L}^1)(\text{pic})]$	402(6000), 386(5400), 339(6600) <sup>s</sup> , 314(7800) <sup>s</sup> , 299(8700) <sup>s</sup>
$[\text{Pd}(\text{L}^2)(\text{pic})]$	406(9000), 386(10 100), 341(11 800) <sup>s</sup> , 312(16 000) <sup>s</sup> , 297(17 500)
$[\text{Pd}(\text{L}^3)(\text{pic})]$	432(3300), 409(3100), 389(2100) <sup>s</sup> , 348(3800) <sup>s</sup> , 326(4700), 258(14 200)

<sup>a</sup> s = shoulder.



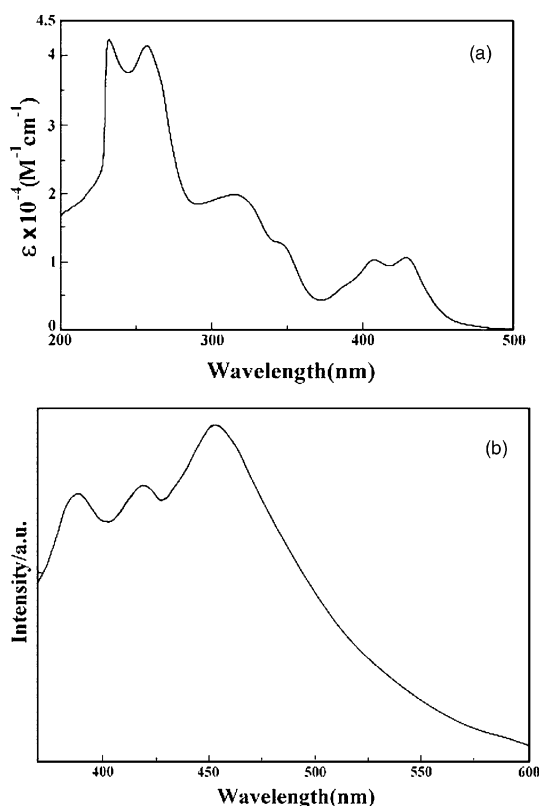


**Fig. 5** (a) Electronic spectrum and (b) emission spectrum of  $[\text{Pd}(\text{L}^3)(\text{PPh}_3)]$  in dichloromethane solution.

$[\text{Pd}(\text{L})(\text{pic})]$  is deposited as Fig. S3.† The compositions of selected molecular orbitals are given in Table 4. In all the cases, the highest occupied molecular orbital (HOMO) has major contributions from the palladium d ( $d_{z^2}$  and  $d_{xy}$ ) orbitals. The lowest unoccupied molecular orbital (LUMO) is delocalized almost entirely on the thiosemicarbazone ligand and is concentrated heavily on the imine ( $\text{C}=\text{N}$ ) fragment. The lower energy absorption in these complexes may therefore be assigned to a charge-transfer transition taking place from the filled palladium d orbital (HOMO) to the vacant

**Table 4** Composition of selected molecular orbitals of the complexes

Compound	Contributing fragments	% contribution of fragments to	
		HOMO	LUMO
$[\text{Pd}(\text{L}^1)(\text{PPh}_3)]$	Pd	89	—
	$\text{L}^1$	7	96 ( $\text{C}=\text{N}$ , 49)
$[\text{Pd}(\text{L}^2)(\text{PPh}_3)]$	Pd	87	—
	$\text{L}^2$	8	93 ( $\text{C}=\text{N}$ , 44)
$[\text{Pd}(\text{L}^3)(\text{PPh}_3)]^a$	Pd	73	—
	$\text{L}^3$	21	97 ( $\text{C}=\text{N}$ , 30)
$[\text{Pd}(\text{L}^1)(\text{pic})]$	Pd	92	—
	$\text{L}^1$	2	93 ( $\text{C}=\text{N}$ , 47)
$[\text{Pd}(\text{L}^2)(\text{pic})]$	pic	—	12
	Pd	90	—
	$\text{L}^2$	6	91 ( $\text{C}=\text{N}$ , 26)
$[\text{Pd}(\text{L}^3)(\text{pic})]^b$	pic	—	44
	Pd	50	—
	$\text{L}^3$	41	95 ( $\text{C}=\text{N}$ , 23)
	pic	—	—

<sup>a</sup> The HOMO-1 has 88% contribution from the metal. <sup>b</sup> The HOMO-1 has 93% contribution from the metal.

$\pi^*(\text{imine})$  orbital of the coordinated thiosemicarbazone ligand (LUMO). Such charge-transfer transition in palladium complexes is, to our knowledge, rare.<sup>14</sup> The electronic spectral properties, as well as features of the molecular orbitals, of the  $[\text{Pd}(\text{L})(\text{pic})]$  complexes are similar to those of the  $[\text{Pd}(\text{L})(\text{PPh}_3)]$  analogues.

The intensities of the charge-transfer transitions in the visible region have tempted us to explore the luminescence properties of these complexes and this has been carried out in dichloromethane solution at ambient temperature (298 K). All six  $[\text{Pd}(\text{L})(\text{D})]$  complexes have been found to display emission in the visible region using an excitation wavelength of  $\sim 350$  nm and a selected spectrum is shown in Fig. 5. Quantum yields ( $\phi$ ) of these emissions have been evaluated (Table 5) with reference to  $[\text{Ru}(\text{bpy})_3]\text{Cl}_2$  ( $\phi = 0.028$  at 298 K).<sup>15</sup> The

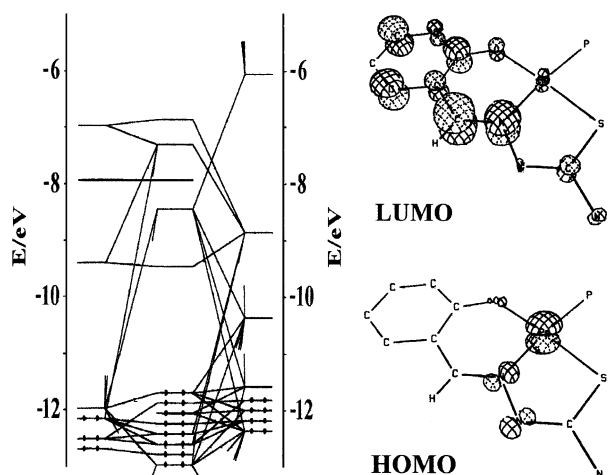


**Fig. 6** Partial molecular orbital diagram of the  $[\text{Pd}(\text{L}^1)(\text{PPh}_3)]$  complex.

**Table 5** Emission spectral data for the complexes

Compound	Emission data		
	$\lambda_{\text{max}}/\text{nm}$		
	Excitation	Emission <sup>a</sup>	Quantum yield ( $\phi$ )
$[\text{Pd}(\text{L}^1)(\text{PPh}_3)]$	340	367 428	$1.17 \times 10^{-3}$
$[\text{Pd}(\text{L}^2)(\text{PPh}_3)]$	340	380 <sup>s</sup> 423	$1.38 \times 10^{-3}$
$[\text{Pd}(\text{L}^3)(\text{PPh}_3)]$	350	382 450	$0.36 \times 10^{-3}$
$[\text{Pd}(\text{L}^1)(\text{pic})]$	339	380 445 <sup>s</sup>	$2.21 \times 10^{-3}$
$[\text{Pd}(\text{L}^2)(\text{pic})]$	341	380 440 478 <sup>s</sup>	$0.83 \times 10^{-3}$
$[\text{Pd}(\text{L}^3)(\text{pic})]$	379	385 450 525	$7.64 \times 10^{-3}$

<sup>a</sup> s = shoulder.

observed quantum yields indicate that these  $[\text{Pd}(\text{L})(\text{PPh}_3)]$  and  $[\text{Pd}(\text{L})(\text{pic})]$  complexes are relatively poor emitters at room temperature.

### Cytotoxicity assay

The *in vitro* growth inhibitory effects of the  $[\text{Pd}(\text{L})(\text{D})]$  complexes were evaluated in two human cell lines *viz.* promyelocytic HL-60 and histiocytic lymphoma U-937. Four human clinical drugs, cisplatin, BCNU, 5-FU and hydroxyurea, were used as reference compounds for comparison. The activities are expressed in terms of  $\text{IC}_{50}$  value, the concentration of the respective compound required to reduce the cell survival fraction to 50% after 72 h of exposure. The lower the  $\text{IC}_{50}$  value is, the greater is the cytotoxicity. From the results presented in Table 6, it is found that the  $[\text{Pd}(\text{L}^1)(\text{PPh}_3)]$  and  $[\text{Pd}(\text{L}^2)(\text{PPh}_3)]$  complexes are much more active than all the clinical drugs, including cisplatin, in HL-60. In U-937,  $[\text{Pd}(\text{L}^2)(\text{PPh}_3)]$  is more active than cisplatin and other reference compounds, while the activity of  $[\text{Pd}(\text{L}^1)(\text{PPh}_3)]$  is higher than BCNU and hydroxyurea, comparable to 5-FU, and less than cisplatin. The  $[\text{Pd}(\text{L}^3)(\text{PPh}_3)]$  complex did not show any appreciable activity in the cell lines. In HL-60, the  $[\text{Pd}(\text{L})(\text{pic})]$  complexes are more active than BCNU, 5-FU and hydroxyurea. The activity of  $[\text{Pd}(\text{L}^1)(\text{pic})]$  is less than cisplatin, while that of the other two complexes is comparable to cisplatin. In U-937 the  $[\text{Pd}(\text{L})(\text{pic})]$  complexes are more active than BCNU and hydroxyurea, and less active than cisplatin and 5-FU.

### In vitro apoptosis assay

Cell death may occur by one of two distinct mechanisms: necrosis or apoptosis. The most common and well-defined form of programmed cell death is apoptosis. During the past decade, cell biology as well as oncology research has focused on apoptosis. Hence, based on the results of our *in vitro* cytotoxicity assay in HL-60, it was thought worthwhile to further explore the apoptotic properties of  $[\text{Pd}(\text{L}^2)(\text{PPh}_3)]$  and  $[\text{Pd}(\text{L})(\text{pic})]$ , the most active members from each group. The apoptosis assay was conducted in HL-60 by the annexin V-FITC/PI method in a flow cytometer after an incubation period of 24 h. The results obtained for the complexes have been compared with those for cisplatin and the well-known apoptosis inducer camptothecin, and are shown in Fig. 7. Each drug treatment was done at 5 and 10  $\mu\text{M}$  concentration. Exposure of cells to cisplatin resulted to 1.39% and 1.20% of gated cells in LR and 3.23% and 6.31% in UR, respectively

**Table 6** Cytotoxicity assay  $\text{IC}_{50}$  values ( $\mu\text{M}$ )<sup>a</sup>

Compound	HL-60	U-937
$[\text{Pd}(\text{L}^1)(\text{PPh}_3)]$	2.5	4.8
$[\text{Pd}(\text{L}^2)(\text{PPh}_3)]$	0.6	1.3
$[\text{Pd}(\text{L}^3)(\text{PPh}_3)]$	203.0	231.6
$[\text{Pd}(\text{L}^1)(\text{pic})]$	16.2	7.3
$[\text{Pd}(\text{L}^2)(\text{pic})]$	7.1	6.6
$[\text{Pd}(\text{L}^3)(\text{pic})]$	6.5	7.7
Cisplatin	7.0	3.2
BCNU	30.5	12.3
5-FU	266.0	4.7
Hydroxyurea	204.0	115.0

<sup>a</sup> For details, see experimental.

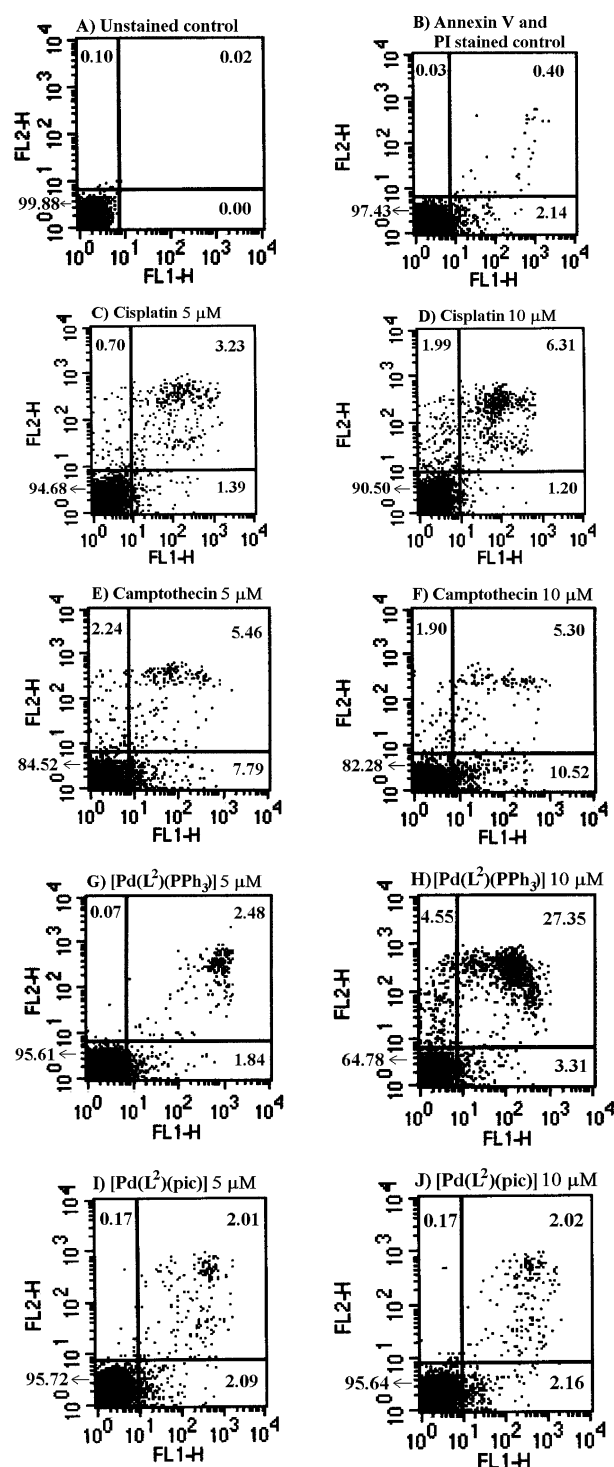


**Fig. 7** Flow cytometric analysis of apoptosis and necrosis in HL-60 cells after treatment with four drugs or complexes at two different concentrations. Quadrant analysis of fluorescence intensity of gated cells in FL-1 and FL-2 channels was from 10 000 events. Figures in the cytogram indicate the percent of gated cells in each quadrant. (FL1-H = annexin V, FL2-H = propidium iodide).

(Fig. 7C and D).<sup>16</sup> Camptothecin induced 7.79% and 10.52% in LR and 5.46% and 5.30% in UR (Fig. 7E and F). The  $[\text{Pd}(\text{L}^2)(\text{PPh}_3)]$  complex exhibited 1.84% and 3.31% in LR and 2.48% and 27.35% in UR (Fig. 7G and H). Thus, it

induces apoptosis to a greater extent than cisplatin as well as camptothecin at 10  $\mu$ M concentration. On the other hand, the  $[\text{Pd}(\text{L}^3)(\text{pic})]$  complex induces 2.09% and 2.16% in LR and 2.01% and 2.02% in UR (Fig. 7I and J).

## Conclusions

The present study shows that salicylaldehyde thiosemicarbazones and similar ligands can smoothly bind to metal ions as tridentate O,N,S-donors, provided an adequate number of coordination sites are readily available on the target metal ion. This study also demonstrates that  $[\text{Pd}(\text{L}^2)(\text{PPh}_3)]$  has remarkable cytotoxic properties among all the compounds tested, including recognized anticancer drugs, which is manifested through the  $\text{IC}_{50}$  values and has been further corroborated by the apoptosis study in HL-60, where it induces apoptosis to a greater extent than cisplatin and camptothecin.

## Experimental

### Materials

Palladium chloride was obtained from Arora Matthey, Kolkata, India, and was converted to  $\text{Na}_2[\text{PdCl}_4]$ .<sup>17</sup> Salicylaldehyde, 2-hydroxyacetophenone and 2-hydroxynaphthaldehyde were obtained from S. D. fine-chem, Mumbai, India. Thiosemicarbazide was procured from Loba Chemie, Mumbai, India. All other chemicals and solvents were reagent grade commercial materials and were used as received. The  $[\text{Pd}(\text{PPh}_3)_2\text{Cl}_2]$  and  $[\text{Pd}(\text{pic})_2\text{Cl}_2]$  complexes were prepared starting from  $\text{Na}_2[\text{PdCl}_4]$  by following reported procedures.<sup>18,19</sup> The thiosemicarbazone ligands ( $\text{H}_2\text{L}^1$ ,  $\text{H}_2\text{L}^2$  and  $\text{H}_2\text{L}^3$ ) were prepared by condensing the respective aldehyde or ketone with thiosemicarbazide in hot ethanol.

### Synthesis

**$[\{\text{Pd}(\text{L}^1)\}_n]$ .** To a solution of  $\text{H}_2\text{L}^1$  (64 mg, 0.33 mmol) in hot ethanol (30 ml), was added triethylamine (66 mg, 0.66 mmol) followed by  $\text{Na}_2[\text{PdCl}_4]$  (100 mg, 0.33 mmol). The mixture was heated at reflux for 6 h. A brown precipitate settled down on cooling, which was collected by filtration, washed with ethanol and dried in air to afford  $[\{\text{Pd}(\text{L}^1)\}_n]$  as a brown powder. Yield: 84 mg (85%). Anal. calc. for  $(\text{C}_8\text{H}_7\text{N}_3\text{SOPd})_n$ : C 31.96; H 2.33; N 13.98. Found: C 31.77; H 2.43; N 14.11%.

The  $[\{\text{Pd}(\text{L}^2)\}_n]$  and  $[\{\text{Pd}(\text{L}^3)\}_n]$  complexes were prepared by following the same above procedure using, respectively,  $\text{H}_2\text{L}^2$  and  $\text{H}_2\text{L}^3$  instead of  $\text{H}_2\text{L}^1$ .

**$[\{\text{Pd}(\text{L}^2)\}_n]$ .** Anal. calc. for  $(\text{C}_9\text{H}_9\text{N}_3\text{SOPd})_n$ : C 34.46; H 2.87; N 13.40. Found: C 34.58; H 2.99; N 13.23%.

**$[\{\text{Pd}(\text{L}^3)\}_n]$ .** Anal. calc. for  $(\text{C}_{12}\text{H}_9\text{N}_3\text{SOPd})_n$ : C 48.82; H 3.62; N 12.66. Found: C 48.67; H 3.77; N 12.87%.

**$[\text{Pd}(\text{L}^1)(\text{PPh}_3)]$ .** **Method A.** The polymeric  $[\{\text{Pd}(\text{L}^1)\}_n]$  species (100 mg) and triphenylphosphine (88 mg) were taken together in ethanol (30 ml) and the solution was refluxed for 24 h to yield a yellow solution. Evaporation of this solution gave a yellow solid, which was subjected to purification by thin layer chromatography on a silica plate. With 1 : 40 acetonitrile–benzene as the eluant, a major yellow band separated,

which was extracted with acetonitrile. Upon evaporation of the acetonitrile extract  $[\text{Pd}(\text{L}^1)(\text{PPh}_3)]$  was obtained as a crystalline yellow solid. Yield: 113 mg (60%).

**Method B.** To a solution of  $\text{H}_2\text{L}^1$  (28 mg, 0.14 mmol) in hot ethanol (30 ml) was added triethylamine (29 mg, 0.29 mmol) followed by  $[\text{Pd}(\text{PPh}_3)_2\text{Cl}_2]$  (100 mg, 0.14 mmol). The mixture was heated at reflux for 5 h to yield a yellow solution. Evaporation of this solution gave a yellow solid, which was subjected to purification by thin layer chromatography on a silica plate. With benzene as the eluant, a yellow band separated, which was extracted with acetonitrile. Upon evaporation of the acetonitrile extract  $[\text{Pd}(\text{L}^1)(\text{PPh}_3)]$  was obtained as a crystalline yellow solid. Yield: 52 mg (65%) Anal. calc. for  $\text{C}_{26}\text{H}_{22}\text{N}_3\text{SOPd}$ : C 55.57; H 3.92; N 7.48. Found: C 55.62; H 3.86; N 7.50%.  $^1\text{H}$  NMR in  $\text{CDCl}_3$   $\delta$ /ppm: 4.76 (s, 2H), 6.62 (t,  $J$  = 7.3 Hz, 1H), 6.68 (d,  $J$  = 8.5 Hz, 1H), 7.22 (t,  $J$  = 7.7 Hz, 1H), 7.31 (d,  $J$  = 8.0 Hz, 1H), 7.41–7.75<sup>20</sup> ( $\text{PPh}_3$ ), 8.24 (d,  $J$  = 12.99 Hz, 1H).

The  $[\text{Pd}(\text{L}^2)(\text{PPh}_3)]$  and  $[\text{Pd}(\text{L}^3)(\text{PPh}_3)]$  complexes were prepared by following the same above procedure using, respectively,  $\text{H}_2\text{L}^2$  and  $\text{H}_2\text{L}^3$  instead of  $\text{H}_2\text{L}^1$ .

**$[\text{Pd}(\text{L}^2)(\text{PPh}_3)]$ .** Anal. calc. for  $\text{C}_{27}\text{H}_{24}\text{N}_3\text{SOPd}$ : C 56.31; H 4.17; N 7.30. Found: C 56.40; H 4.23; N 7.33%.  $^1\text{H}$  NMR in  $\text{CDCl}_3$   $\delta$ /ppm: 2.89 (s, 3H), 4.78 (s, 2H), 6.62 (d,  $J$  = 8.34 Hz, 1H), 6.68 (t,  $J$  = 7.6 Hz, 1H), 7.17 (t,  $J$  = 7.7 Hz, 1H), 7.43–7.72<sup>20</sup> ( $\text{PPh}_3$ ), 7.62 (d,  $J$  = 1.4 Hz, 1H).

**$[\text{Pd}(\text{L}^3)(\text{PPh}_3)]$ .** Anal. calc. for  $\text{C}_{30}\text{H}_{24}\text{N}_3\text{SOPd}$ : C 58.88; H 3.93; N 6.87. Found: C 58.86; H 3.88; N 6.94%.  $^1\text{H}$  NMR in  $\text{CDCl}_3$   $\delta$ /ppm: 4.83 (s, 2H), 6.76 (d,  $J$  = 9.2 Hz, 1H), 7.32 (t,  $J$  = 5.6 Hz, 1H), 7.50–7.83<sup>20</sup> (m, 15H ( $\text{PPh}_3$ ) and t, 1H), 8.11 (d,  $J$  = 8.5 Hz, 1H), 9.52 (d,  $J$  = 13.2 Hz, 1H).

**$[\text{Pd}(\text{L}^1)(\text{pic})]$ .** **Method A.** The polymeric  $[\{\text{Pd}(\text{L}^1)\}_n]$  species (100 mg) and 4-picoline (31 mg) were taken in ethanol (30 ml) and the solution was refluxed for 24 h to yield a yellow solution. Evaporation of this solution gave a yellow solid, which was subjected to purification by thin layer chromatography on a silica plate. With 1 : 20 acetonitrile–benzene as the eluant, a prominent yellow band separated, which was extracted with acetonitrile. Upon evaporation of the acetonitrile extract  $[\text{Pd}(\text{L}^1)(\text{pic})]$  was obtained as a crystalline yellow solid. Yield: 66 mg (50%).

**Method B.** To a solution of  $\text{H}_2\text{L}^1$  (54 mg, 0.28 mmol) in hot ethanol (30 ml) was added triethylamine (56 mg, 0.55 mmol) followed by  $[\text{Pd}(\text{pic})_2\text{Cl}_2]$  (100 mg, 0.28 mmol). The mixture was heated at reflux for 6 h to yield a yellow solution. Evaporation of this solution gave a yellow solid, which was subjected to purification by thin layer chromatography on a silica plate. With 1 : 20 acetonitrile–benzene as the eluant, a major yellow band separated, which was extracted with acetonitrile. Upon evaporation of the acetonitrile extract  $[\text{Pd}(\text{L}^1)(\text{pic})]$  was obtained as a crystalline yellow solid. Yield: 59 mg (55%). Anal. calc. for  $\text{C}_{14}\text{H}_{14}\text{N}_4\text{SOPd}$ : C 42.56; H 3.42; N 14.29. Found: C 42.38; H 3.45; N 14.23%.  $^1\text{H}$  NMR in  $\text{CDCl}_3$   $\delta$ /ppm: 2.44 (s, 3H), 4.87 (s, 2H), 6.67 (t,  $J$  = 7.3 Hz, 1H), 7.03 (d,  $J$  = 8.8 Hz, 1H), 7.24 (d,  $J$  = 5.7 Hz, 2H), 7.29–7.34<sup>20</sup> (2H), 7.92 (s, 1H), 8.62 (d,  $J$  = 5.9 Hz, 2H).

The  $[\text{Pd}(\text{L}^2)(\text{pic})]$  and  $[\text{Pd}(\text{L}^3)(\text{pic})]$  complexes were prepared by following the same above procedure using, respectively,  $\text{H}_2\text{L}^2$  and  $\text{H}_2\text{L}^3$  instead of  $\text{H}_2\text{L}^1$ .

**$[\text{Pd}(\text{L}^2)(\text{pic})]$ .** Anal. calc. for  $\text{C}_{15}\text{H}_{16}\text{N}_4\text{SOPd}$ : C 44.29; H 3.94; N 13.78. Found: C 44.44; H 3.86; N 13.76%.  $^1\text{H}$  NMR in  $\text{CDCl}_3$   $\delta/\text{ppm}$ : 2.43 (s, 3H), 2.75 (s, 3H), 4.84 (s, 2H), 6.68 (t,  $J = 7.3$  Hz, 1H), 7.04 (d,  $J = 8.2$  Hz, 1H), 7.21–7.26<sup>20</sup> (3H), 7.68 (d,  $J = 8.2$  Hz, 1H), 8.61 (d,  $J = 6.2$  Hz, 1H).

**$[\text{Pd}(\text{L}^3)(\text{pic})]$ .** Anal. calc. for  $\text{C}_{18}\text{H}_{16}\text{N}_4\text{SOPd}$ : C 48.82; H 3.62; N 12.66. Found: C 48.99; H 3.78; N 12.45%.  $^1\text{H}$  NMR in  $\text{CDCl}_3$   $\delta/\text{ppm}$ : 2.45 (s, 3H), 4.87 (s, 2H), 7.13–7.26<sup>20</sup> (4H), 7.48 (d,  $J = 7.44$  Hz, 1H), 7.69–7.50<sup>20</sup> (2H), 8.06 (d,  $J = 8.5$  Hz, 1H), 8.65 (d,  $J = 2.5$  Hz, 2H), 8.93 (s, 1H).

### Cytotoxicity assay

**Cell lines and culture.** HL-60 and U-937 (purchased from National Center for Cell Sciences, Pune, India) were maintained in complete sterile growth medium RPMI-1640 with L-glutamine (GIBCO, Invitrogen Corporation, USA), containing 10% heat inactivated fetal bovine serum (GIBCO, Invitrogen Corporation, USA) and 1% antibiotics [10 000 U penicillin  $\text{mL}^{-1}$  and 10 000  $\mu\text{g}$  streptomycin  $\text{mL}^{-1}$ , BioWhittaker, Cambrex Bio Science, USA]. Cell cultures were maintained in log phase using a subculture ratio of 1 : 5 twice a week.

**Preparation of test material.** Working stock solutions of all the compounds were prepared by dissolving 20 mg of each compound in 1 ml of DMSO [Hybri-Max grade, Sigma-Aldrich Co., USA] and filtered under sterile conditions. These were serially diluted with complete RPMI-1640 medium prior to use to obtain different drug concentrations.

**MTT-based cytotoxicity test.** 100  $\mu\text{L}$  of cell suspension from the stock  $2 \times 10^5$  HL-60 or  $1 \times 10^5$  U-937 cells  $\text{mL}^{-1}$  were added to 96-well cell culture plates. Next, 10  $\mu\text{L}$  of drug solutions of different concentrations were added to respective wells followed by the addition of the medium (90  $\mu\text{L}$ ) in triplicate (total volume 200  $\mu\text{L}$ /well). All vehicle controls contained the same concentration of DMSO. Plates were incubated for 72 h at 37 °C, 5%  $\text{CO}_2$ –95% air with humidity. After removal of 100  $\mu\text{L}$  of media from each well, 10  $\mu\text{L}$  of a 5 mg  $\text{mL}^{-1}$  solution of 3-(4,5-dimethylthiazol-2-yl)-2,5-diphenyltetrazolium bromide [MTT, Sigma, USA] in Dulbecco's PBS (GIBCO, BRL) were added to each well and the plate was incubated for 4 h at 37 °C. Subsequently 100  $\mu\text{L}$  of acidic isopropanol solution (0.04 N HCl in isopropanol) was added to the wells to dissolve formed formazan crystals. The plate was read in a microplate reader (Bio-Rad, USA, Model 550) at 540 nm. The percentage cell viability was calculated by dividing the average absorbance of the cells treated with compounds by that of the control;  $\text{IC}_{50}$  (drug concentration needed for 50% inhibition of cells relative to control) was determined through Curvefit software by plotting % inhibition vs. drug concentration and expressed in  $\mu\text{M}$  concentration.

### In vitro apoptosis assay

Induction of apoptosis *in vitro* by two representative complexes of each type  $[\text{Pd}(\text{L})(\text{D})]$  (when  $\text{D} = \text{PPh}_3$  and pic), cisplatin and camptothecin were determined by a flow cytometric assay using an annexin V-FITC<sup>21</sup> apoptosis detection kit (BD Biosciences Pharmingen, San Diego, USA). Exponentially growing HL-60 cells in complete RPMI-1640 media (100  $\mu\text{L}$  of  $5 \times 10^6$ ) were plated in six well plates. 10  $\mu\text{L}$  of each compound in DMSO (5 and 10  $\mu\text{M}$  concentrations) was added to the wells followed by the addition of required media (total volume 1 ml). Plates were incubated at 37 °C for 24 h. The cells were centrifuged at room temperature at 1500 rpm for 5 min. The pellet was washed twice with cold PBS and re-suspended in the binding buffer (1X, 100  $\mu\text{L}$ ) provided in the kit. The cells were stained with annexin V-FITC (5  $\mu\text{L}$ ) and propidium iodide [PI] (5  $\mu\text{L}$ ) and incubated for 15 min in the dark at 25 °C. Next, 400  $\mu\text{L}$  of binding buffer was added to each tube and analyzed on a FACScan flow cytometer (Becton Dickinson, Mountainview, CA) using Cell Quest software. Two controls, *viz.* unstained cells and cells stained with both annexin V-FITC and PI, containing DMSO as vehicle were used. Cells that were annexin<sup>+</sup>/PI<sup>−</sup> and annexin<sup>+</sup>/PI<sup>+</sup> were considered positive for apoptosis.

### Physical measurements

Microanalyses (C, H, N) were performed using a Heraeus Carlo Erba 1108 elemental analyzer. IR spectra were obtained on a Shimadzu FTIR-8300 spectrometer with samples prepared as KBr pellets. Electronic spectra were recorded on a JASCO V-570 spectrophotometer. Emission spectra were recorded on a Perkin Elmer LS55 luminescence spectrometer.  $^1\text{H}$  NMR spectra were recorded in  $\text{CDCl}_3$  solutions on a

**Table 7** Crystallographic data for  $[\text{Pd}(\text{L}^1)(\text{PPh}_3)]$  and  $[\text{Pd}(\text{L}^2)(\text{pic})]$

	$[\text{Pd}(\text{L}^1)(\text{PPh}_3)]$	$[\text{Pd}(\text{L}^2)(\text{pic})]$
Empirical formula	$\text{C}_{26}\text{H}_{22}\text{N}_3\text{OPSPd}$	$\text{C}_{15}\text{H}_{16}\text{N}_4\text{OSPd}$
Formula mass	561.9	406.78
Crystal system	Triclinic	Orthorhombic
Space group	<i>P1</i>	<i>Pbca</i>
<i>a</i> / $\text{\AA}$	7.5385(4)	8.3942(12)
<i>b</i> / $\text{\AA}$	10.2179(5)	15.149(2)
<i>c</i> / $\text{\AA}$	16.9756(9)	25.099(4)
$\alpha/^\circ$	77.025(1)	90
$\beta/^\circ$	80.819(1)	90
$\gamma/^\circ$	71.567(1)	90
<i>V</i> / $\text{\AA}^3$	1203.27(11)	3191.7(8)
<i>Z</i>	2	8
<i>D</i> <sub>calc</sub> /mg $\text{m}^{-3}$	1.551	1.693
<i>F</i> (000)	568	1632
$\lambda/\text{\AA}$	0.71073	0.71073
Crystal size/ $\text{mm}^3$	$0.38 \times 0.30 \times 0.15$	$0.12 \times 0.28 \times 0.48$
<i>T</i> /K	295(2)	298
$\mu/\text{mm}^{-1}$	0.948	1.3
Independent reflections	5525	3135
<i>R</i> <sub>int</sub>	0.0261	0.022
Collected reflections	15972	30751
<i>R</i> <sub>1</sub> <sup>a</sup>	0.026	0.0219
<i>wR</i> <sub>2</sub> <sup>b</sup>	0.0702	0.0595
GOF <sup>c</sup>	1.159	1.076

<sup>a</sup>  $R_1 = \sum ||F_o| - |F_c|| / \sum |F_o|$ . <sup>b</sup>  $wR_2 = [\sum [w(F_o^2 - F_c^2)^2] / \sum [w(F_o^2)^2]]^{1/2}$ . <sup>c</sup> GOF =  $[\sum [w(F_o^2 - F_c^2)^2] / (M - N)]^{1/2}$ , where *M* is the number of reflections and *N* is the number of parameters refined.



Bruker Avance DPX 300 NMR spectrometer using TMS as the internal standard.

### X-Ray crystallography

Single crystals of  $[\text{Pd}(\text{L}^1)(\text{PPh}_3)]$  and  $[\text{Pd}(\text{L}^2)(\text{pic})]$  were grown by slow evaporation of 1 : 1 dichloromethane–acetonitrile solutions of the respective compounds. Selected crystal data and data collection parameters are given in Table 7. Data on the crystals were collected on a BRUKER SMART ApexCCD area detector. A total 15 972 and 30 571 reflections giving 5525 and 3135 unique reflections were collected ( $R_{\text{int}} = 0.0261$  and 0.022) for  $[\text{Pd}(\text{L}^1)(\text{PPh}_3)]$  and  $[\text{Pd}(\text{L}^2)(\text{pic})]$ , respectively. X-Ray data reduction, structure solution and refinement were done using the SHELXS-97 and SHELXL-97 packages.<sup>22</sup> The structures were solved by direct methods.

CCDC reference numbers 646551 and 646552. For crystallographic data for the  $[\text{Pd}(\text{L})(\text{PPh}_3)]$  and  $[\text{Pd}(\text{L})(\text{pic})]$  complexes in CIF or other electronic format see DOI: 10.1039/b707448d

### Acknowledgements

Financial assistance received from the Council of Scientific and Industrial Research, New Delhi, India, [grant no. 01(1952)/04/EMR-II] is gratefully acknowledged. The authors thank the anonymous referees for their constructive criticisms and suggestions, which have been of great help in preparing the revised manuscript. Sincere thanks are due to Prof. Chittaranjan Sinha and Dr Asok Nath Mandal of the Department of Chemistry, Jadavpur University, for their help with the fluorescence and NMR spectral measurements, respectively. Sincere thanks are also due to Dr Golam Mostafa of the Department of Physics, Jadavpur University, for his help in resolving some crystallographic queries. The authors are grateful to Dr Jaydip Biswas, Director, Chittaranjan National Cancer Institute, for his encouragement and Dr R. N. Baral, In-Charge, Department of Immunoregulation & Immunodiagnostics, for helpful discussions. Sarmistha Halder thanks the University Grants Commission, New Delhi, India, for her fellowship [grant no. 10-2(5)2004(1)-E.U.II].

### References

- (a) M. J. M. Campbell, *Coord. Chem. Rev.*, 1975, **15**, 279; (b) S. B. Padhye and G. B. Kaffman, *Coord. Chem. Rev.*, 1985, **63**, 127; (c) I. Haiduc and C. Silvestru, *Coord. Chem. Rev.*, 1990, **99**, 253; (d) D. X. West, S. B. Padhye and P. B. Sonawane, *Struct. Bonding*, 1992, **76**, 1; (e) D. X. West, A. E. Liberta, S. B. Padhye, R. C. Chikate, P. B. Sonawane, A. S. Kumbhar and R. G. Yerande, *Coord. Chem. Rev.*, 1993, **123**, 49; (f) J. R. Dilworth, P. Amold, D. Morales, Y. L. Wong and Y. Zheng, *Mod. Coord. Chem.*, 2002, 217; (g) A. G. Quiroga and C. N. Raninger, *Coord. Chem. Rev.*, 2004, **248**, 119.
- (a) Z. Iakovidou, A. Papageorgiou, M. A. Demertzis, E. Mioglou, D. Mourelatos, A. Kotsis, P. N. Yadav and D. Kovala-Demertzi, *Anti-Cancer Drugs*, 2001, **12**, 65; (b) J. Patole, S. Dutta, S. Padhye and E. Sinn, *Inorg. Chim. Acta*, 2001, **318**, 207; (c) R. I. Maurer, P. J. Blower, J. R. Dilworth, C. A. Reynolds, Y. Zheng and G. E. D. Mullen, *J. Med. Chem.*, 2002, **45**, 1420; (d) A. R. Cowly, J. R. Dilworth, P. S. Donnelly, E. Labisbal and A. Sousa, *J. Am. Chem. Soc.*, 2002, **124**, 5270; (e) M. B. Ferrari, F. Bisceglie, G. Pelosi, M. Sassi, P. Tarasconi, M. Cornia, S. Capacchi, R. Albertini and S. Pinelli, *J. Inorg. Biochem.*, 2002, **90**, 113; (f) E. M. Jouad, X. D. Thanh, G. Bouet, S. Bonneau and M. A. Khan, *Anticancer Res.*, 2002, **22**, 1713; (g) S. Padhye, Z. Afrasiabi, E. Sinn, J. Fok, K. Mehta and N. Rath, *Inorg. Chem.*, 2005, **44**, 1154; (h) J. Ruiz, N. Cutillas, C. Vicente, M. D. Villa, G. López, J. Lorenzo, F. X. Avilés, V. Moreno and D. Bautista, *Inorg. Chem.*, 2005, **44**, 7365.
- Y. P. Tion, C. Y. Duan, Z. L. Lu, X. Z. You, H. K. Fun and S. Kandasamy, *Polyhedron*, 1996, **15**, 2263.
- (a) A. De Bolfo, T. D. Smith, J. F. Boas and J. R. Pilbrow, *Aust. J. Chem.*, 1976, **29**, 2583; (b) Z. Lu, C. White, A. L. Rheingold and R. H. Crabtree, *Inorg. Chem.*, 1993, **32**, 3991; (c) D. X. West, Y.-H. Yang, T. L. Klein, K. I. Goldberg, A. E. Liberta, J. Valdés-Martínez and R. A. Toscano, *Polyhedron*, 1995, **14**, 1681; (d) D. X. West, Y.-H. Yang, T. L. Klein, K. I. Goldberg, A. E. Liberta, J. Valdés-Martínez and S. Hernández-Ortega, *Polyhedron*, 1995, **14**, 3051; (e) P. Souza, I. A. Matesanz and V. Fernandez, *J. Chem. Soc., Dalton Trans.*, 1996, 3011; (f) D. Kovala-Demertzi, A. Domopoulou, M. A. Demertzis, J. Valdés-Martínez, S. Hernández-Ortega, G. Espinosa-Pérez, D. X. West, M. M. Salberg, G. A. Bain and P. D. Bloom, *Polyhedron*, 1996, **15**, 2587; (g) M. A. Ali, K. K. Dey, M. Nazimuddin, F. E. Smith, R. J. Butcher, J. P. Jasinski and J. M. Jasinski, *Polyhedron*, 1996, **15**, 3331.
- (a) D. Kovala-Demertzi, N. Kourkoumelis, M. A. Demertzis, J. R. Miller, C. S. Frampton, J. K. Swearingen and D. X. West, *Eur. J. Inorg. Chem.*, 2000, 727; (b) P. N. Yadav, M. A. Demertzis, D. Kovala-Demertzi, A. Castiñeiras and D. X. West, *Inorg. Chim. Acta*, 2002, **332**, 204.
- F. Basuli, S.-M. Peng and S. Bhattacharya, *Inorg. Chem.*, 1997, **36**, 5645.
- (a) A. Castiñeiras, E. Bermejo, D. X. West, A. K. El-Sawaf and J. K. Swearingen, *Polyhedron*, 1998, **17**, 2751; (b) A. Castiñeiras, M. Gil, E. Bermejo and D. X. West, *Z. Naturforsch., B: Chem. Sci.*, 2000, **55**, 863; (c) E. Bermejo, A. Castiñeiras, L. J. Ackerman, M. D. Owens and D. X. West, *Z. Anorg. Allg. Chem.*, 2001, **627**, 1966; (d) C. A. Brown, W. Kaminsky, K. A. Claborn, K. I. Goldberg and D. X. West, *J. Braz. Chem. Soc.*, 2002, **13**, 10.
- I. Pal, F. Basuli, T. C. W. Mak and S. Bhattacharya, *Angew. Chem., Int. Ed.*, 2001, **40**, 2923.
- (a) F. Basuli, M. Ruf, C. G. Pierpont and S. Bhattacharya, *Inorg. Chem.*, 1998, **39**, 6113; (b) F. Basuli, S.-M. Peng and S. Bhattacharya, *Inorg. Chem.*, 2000, **39**, 1120; (c) S. Dutta, F. Basuli, S. M. Peng, G. H. Lee and S. Bhattacharya, *New J. Chem.*, 2002, **26**, 1607; (d) R. Acharyya, S. Dutta, F. Basuli, S. M. Peng, G. H. Lee, L. R. Falvello and S. Bhattacharya, *Inorg. Chem.*, 2006, **45**, 1252; (e) S. Basu, R. Acharyya, W. S. Sheldrick, H. Mayer-Figge and S. Bhattacharya, *Struct. Chem.*, 2007, **18**, 209.
- (a) L. Adrio, G. Alberdi, A. Amoedo, D. Lata, A. Fernández, J. Martínez, M. T. Pereira and J. M. Vila, *Z. Anorg. Allg. Chem.*, 2005, **631**, 2204; (b) J. L. Neto, G. M. Lima and H. Beraldo, *Spectrochim. Acta, Part A*, 2006, **62**, 669; (c) A. R. Jalilian, M. Sadeghi, Y. Y. Kamrani and M. R. Ensaf, *J. Radioanal. Nucl. Chem.*, 2006, **268**, 605; (d) L. Otero, M. Vieites, L. Boiani, A. Denicola, C. Rigol, L. Opazo, C. Olea-Azar, J. D. Maya, A. Morello, R. L. Krauth-Siegel, O. E. Piro, E. Castellano, M. González, D. Gambino and H. Cerecetto, *J. Med. Chem.*, 2006, **49**, 3322; (e) J. Martínez, L. A. Adrio, J. M. Antelo, J. M. Ortigueira, M. T. Pereira, J. J. Fernández, A. Fernández and J. M. Vila, *J. Organomet. Chem.*, 2006, **691**, 2721; (f) J. Martínez, L. A. Adrio, J. M. Antelo, J. M. Ortigueira, M. T. Pereira, M. López-Torres and J. M. Vila, *J. Organomet. Chem.*, 2006, **691**, 2891; (g) A. Amoedo, L. A. Adrio, J. M. Antelo, J. Martínez, M. T. Pereira, A. Fernández and J. M. Vila, *Eur. J. Inorg. Chem.*, 2006, 3016; (h) N. I. Dodoff, D. Kovala-Demertzi, M. Kubiak, J. Kuduk-Jaworska, A. Kochel and G. A. Gorneva, *Z. Naturforsch., B: Chem. Sci.*, 2006, **61**, 1110; (i) M. A. Demertzis, P. N. Yadav and D. Kovala-Demertzi, *Helv. Chim. Acta*, 2006, **89**, 1959; (j) J. Martínez, L. A. Adrio, J. M. Antelo, M. T. Pereira, J. J. Fernández and J. M. Vila, *Polyhedron*, 2006, **25**, 2848; (k) A. R. Jalilian, M. Sadeghi and Y. Y. Kamrani, *Radiochim. Acta*, 2006, **94**, 865; (l) A. I. Matesanz, C. Pastor and P. Souza, *Inorg. Chem. Commun.*, 2007, **10**, 97; (m) A. I. Matesanz and P. Souza, *J. Inorg. Biochem.*, 2007, **101**, 245.
- (a) S. K. Burley and G. A. Petsko, *Adv. Protein Chem.*, 1998, **39**, 125; (b) M. Nishio, M. Hirota and Y. Umezawa, *The CH- $\pi$  interactions (Evidence, Nature and Consequences)*, Wiley-VCH, New York, 1998; (c) Y. Umezawa, S. Tsuboyama, K. Honda, J. Uzawa and M. Nishio, *Bull. Chem. Soc. Jpn.*, 1998, **71**, 1207; (d) G. R. Desiraju and T. Steiner, *The Weak Hydrogen Bond*, IUCr

- Monograph on Crystallography 9*, Oxford University Press, Oxford, 1999; (e) M. J. Hannon, C. L. Painting and N. W. Alcock, *Chem. Commun.*, 1999, 2023; (f) B. J. Mcnelis, L. C. Nathan and C. J. Clark, *J. Chem. Soc., Dalton Trans.*, 1999, 1831; (g) K. Biradha, C. Seward and M. J. Zaworotko, *Angew. Chem., Int. Ed.*, 1999, **38**, 492; (h) M. J. Calhorda, *Chem. Commun.*, 2000, 801; (i) C. Janiak, S. Temizdemir and S. Dechert, *Inorg. Chem. Commun.*, 2000, **3**, 271; (j) C. Janiak, S. Temizdemir, S. Dechert, W. Deck, F. Girgsdies, J. Heinze, M. J. Kolm, T. G. Scarmann and O. M. Zipffel, *Eur. J. Inorg. Chem.*, 2000, 1229.
- 12 (a) S. B. Halligudi, K. N. Bhatt, N. H. Khan, R. I. Kurashy and K. Venkatesubramanian, *Polyhedron*, 1996, **15**, 2093; (b) G. Zhao, H. Lin, P. Yu, H. Sun, S. Zhu, X. Su and Y. Chen, *J. Inorg. Biochem.*, 1999, **73**, 145; (c) B. Milani, A. Scarel, E. Zangrando, G. Mestroni, C. Carfagna and B. Binotti, *Inorg. Chim. Acta*, 2003, **350**, 592.
  - 13 (a) C. Mealli and D. M. Proserpio, *CACAO Version 4.0*, Firenze, Italy, July 1994; (b) C. Mealli and D. M. Proserpio, *J. Chem. Educ.*, 1990, **67**, 399.
  - 14 (a) Y. Shimazaki, M. Tashiro, T. Motoyama, S. Iwatsuki, T. Yajima, Y. Nakabayashi, Y. Naruta and O. Yamauchi, *Inorg. Chem.*, 2005, **44**, 6044; (b) N. D. Jones, P. Meessen, U. Losehand, B. O. Patrick and B. R. James, *Inorg. Chem.*, 2005, **44**, 3290.
  - 15 (a) G. A. Crosby and W. H. Elfring, Jr, *J. Phys. Chem.*, 1976, **80**, 2206; (b) M. J. Cook, A. P. Lewis, G. S. J. Thomson, J. L. Glasper and D. J. Robbins, *J. Chem. Soc., Perkin Trans. 2*, 1984, 293.
  - 16 Abbreviations used: LR (lower right quadrant, representing early apoptotic cells, which are annexin V<sup>+</sup>/PI<sup>-</sup>); UR (upper right quadrant, representing late apoptotic cells, which are annexin V<sup>+</sup>/PI<sup>+</sup>).
  - 17 F. R. Hertley, in *The Chemistry of Palladium and Platinum*, ed. P. L. Robinson, Applied Science, London, 1973, vol. 14, pp. 458.
  - 18 H. L. Grube, in *Handbook of Preparative Inorganic Chemistry*, ed. G. Brauer, Academic Press, London, 2nd edn, 1965, vol. 2, pp. 1584.
  - 19 (a) P. Chattopadhyay and S. K. Majumdar, *Indian J. Chem., Sect. A: Inorg., Bio-inorg., Phys., Theor. Anal. Chem.*, 1983, **22**, 1603; (b) T. K. Thokdar, A. Sarkar, P. K. Paria and S. K. Majumdar, *Indian J. Chem., Sect. A: Inorg., Bio-inorg., Phys., Theor. Anal. Chem.*, 1989, **28**, 181.
  - 20 Overlapping signals.
  - 21 I. Vermes, C. Hannen, H. Steffens-Nakken and C. Reutelingsperger, *J. Immunol. Methods*, 1995, **184**, 39.
  - 22 G. M. Sheldrick, *SHELXS-97, Program for solution of crystal structures*, University of Göttingen, Germany, 1997; G. M. Sheldrick, *SHELXL-97, Program for refinement of crystal structures*, University of Göttingen, Germany, 1997.